ANALYSIS OF THREE IMPELLER FAILURES: EXPERIMENTAL TECHNIQUES USED TO ESTABLISH CAUSES

by

Charles Bultzo

Engineering Associate

Exxon Company, U.S.A.

Baytown, Texas

Charles Bultzo is an Engineering Associate in the Technical Division of of the Exxon Company, U.S.A., Baytown, Texas. He has served as a discussion leader at two of the past turbomachinery symposiums. He has presented nine papers on turbomachinery related subjects to ASME and other technical societies. Mr. Bultzo has been engaged in turbomachinery failure analysis and project development for the past 15 years.

ABSTRACT

Three first-stage impellers have failed in catalytic wet gas service. Two of the failed impellers were made of K-Monel material; the third was made of SAE 4330 material. In the first two cases, the structural integrity of the material was suspect. There was no question about the material in the third case. In all three cases, fatigue appeared to be the common mode of failure. This paper deals with the experimental techniques used in the field and laboratory to help qualify actual stress levels and identify the forcing function that resulted in fatigue.

BACKGROUND

Early in October of 1971, two centrifugal compressors were put into catalytic wet gas service at Exxon's Baytown Refinery replacing two 13-year-old compressors. They were designed to operate with a suction pressure of 22.7 psia while discharging at 190 psia. The design molecular weight was 42. Low alloy steel (4140) had been used with limited success in the original compressors. However, since K-Monel has been used successfully for the last 12 years at this location and 18 years at another location; it was selected for the impeller material. The original plan provided for intercooling; however, due to a continuing problem of carry-over and the resultant fouling and corrosion on the old compressors, the final configuration utilized a hairpin that directed the flow from the interstage outlet to the interstage return nozzle. This was necessary since the casings had already been cast when the decision to eliminate the intercooling was made. The compressors had five impellers with a maximum continuous speed of 8,525 rpm. Performance tests of each machine after being put into service indicated a capacity of approximately 10 percent above the design point without compromise of efficiency while operating with a slightly lower molecular weight gas (41). Overall performance (horsepower/efficiency) was well within that predicted in the original quotation.

The general arrangement of the two compressors relative to their common suction drum and recycle facilities is shown on Figure 1. It should be noted that each compressor has its own line from the suction drum. This configuration was used for two reasons: (1) to reduce the possibility of surge on one machine if the speed increased suddenly on the other and (2) to more uniformly distribute the velocity profile across the internal demister when both compressors were in operation. By definition of service, the gas is near its dew point. Numerous flash calculations made on the gas indicated that at the inlet to the compressor the gas was within 10 degrees of its saturation temperature. It is not unlikely that despite this theoretical approach to superheat that a very fine mist of liquid would be entrained in the gas stream.

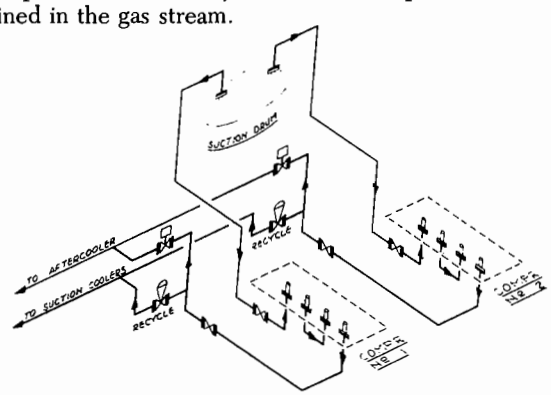

Figure 1. Wet Gas Compressors Piping Arrangement.

After approximately 12 calendar months of operation, we experienced a catastrophic failure of the first-stage impellers on Compressor No. 1. The other four impellers were damaged so severely that their reuse was not possible. Also, substantial damage was sustained by the stator parts. Approximately a month later, a similar failure occurred on Compressor No. 2 with similar consequences. As shown on Table I below, the compressors had been in actual service 282 and 287 days respectively.

Table I
Operating History

	Compressor No. 1	Compressor No. 2
Date In Service	10-5-71	10-27-71
Date of Failure	10-10-72	11-6-72
On-Line Time (Days)	282	287
Number Of Starts	21*	15*

*Because of a fouling problem resulting from solids contained in the steam being used by the turbine drivers, it was necessary to shut down the compressors frequently to permit water washing of the steam turbines. Both compressors had split-line leakage and had to be opened in the field. (Compressor No. 2 was opened twice.) This later commentary is offered to reconcile the on-line time with the in-service and failure dates.

After the first failure occurred, the rotor was removed and a spare rotor was installed. The damaged rotor was returned to the vendor for appraisal as to the cause of failure. After the second failure, it was suggested that the vendor consider the utilization of a third party to help expedite the identification of the cause of the failures. Concurrently, Exxon, with aid from its research facility, would work the problem independently and then submit an analysis of the cause of the failure to the vendor. In the meantime, it was agreed that because of the tip speeds that were being used (934 feet per second, which was high for our Refinery at that time), the replacement rotor should have one stage added. There was ample room in the casing to make this accommodation. The addition of the stage reduced the maximum continuous speed by 1,000 rpm and resulted in a reduction of the tip speed to 822 feet per second. Material availability dictated that the impellers for the new rotor with six stages would be fabricated from SAE 4330 material with a yield of 90,000 psi maximum tensile strength.

METALLURGICAL REVIEW

Both the vendor and Exxon's research facility made independent analysis of the metallurgy of the second failed impeller. The vendor reported yield strengths approximately 33 percent higher than that observed by our facility. (This included in-house and "third party" use of microtensile specimens.) As shown on Figure 2, a scanning electron microscopic fractographic examination of a crack that was in progress and opened for examination indicated the presence of both fatigue and corrosion products. It was Exxon's position that the failure was due to the following:

1. The physical properties of the material were below design.
2. With a high base stress and some forcing function that added a substantial stress over a brief period, fatigue had occurred during the period of the abnormally higher stress. As the crack progressed, the opened surfaces were subjected to a light corrosive attack.

Figure 2. Scanning Electron Microscopic Fractographic Examination of a Crack.

The vendor took the position that admittedly fatigue was present; however, it had concluded that corrosion took place first that set up stress risers, which, in the presence of a forcing function, caused the material to fatigue. Although there was disagreement as to order of events, fatigue was accepted as the mode of failure. Since the catastrophic failure had not occurred immediately after start-up, it was concluded that a change in the operating environment for discrete periods of time must have precipitated the failures. Unfortunately, no attempt was made to identify this forcing function during the exchange of views.

FIELD STRESS ANALYSIS

In an attempt to better understand the actual stress levels being experienced in the failed impellers, the third first-stage impeller, which was part of the original and was also made of K-Monel, was also removed from its rotor and subjected to a series of tests. This included mounting strain gauges to indicate radial and tangential strains as the impeller was being rotated. The mounting of the gauges is shown on Figure 3. To insure that proper techniques were employed, the first set of strain gauges was installed by a consulting firm to insure maximum credibility of the resulting data. A telemetry system was used to transmit the strain from the gauges to a receiver to permit actual rotation of the impeller as shown on Figure 4. After the strain gauges had been put in place, the impeller was mounted on a motor shaft. A plug was installed at the impeller eye to reduce the air flow during the test. The motor was designed for 2,300 volts, but was tied into the 440-volt system. This permitted slow acceleration during the start-up. The complete test setup is shown on Figure 5. Because of the mass of the impeller and the low voltage, a maximum speed of only 2,700 rpm was reached. This represented approximately 32 percent of the maximum continuous speed of the impeller. However, as shown on Figure 6, a plot of the microstrain versus speed showed that this relationship followed a predictable path. The lower speed also enhanced credibility of the data by lessening the mass effect of the interconnecting wire and strain gauges, which might affect the results obtained. Because the impeller was being rotated in open air, there was no heating thus negating strain resulting from temperature gradients despite temperature compensation. As can be seen from Table II, the extrapolated stress level was substantially above that which had been predicted by not only our in-house impeller computer analysis program, but also the vendor's calculations.

Table II

Comparison of Maximum Stress Levels
In First Impeller

	Stress, psi	Location of Maximum Stress
In-House Computer Analysis	72,000	Impeller Eye
Vendor Predicted Stress Level	67,000	Impeller Eye
Strain Gauge Extrapolated To Design, rpm	99,000	In Cover Over Vane 1/2-Inch Out From Fillet At Impeller Eye Over The Nose of The Vane

The extrapolated stress level was approximately 47 percent higher than that predicted by the vendor. Since there was commonality in the predicted stress analysis by both Exxon's system and the vendor's system, it gave rise to the credibility of known computer programs used for the evaluation of stress analysis in impellers. Historically, it has been assumed that the highest stress would occur at the impeller eye. However, this test and subsequent tests on the second-stage impeller from this rotor and smaller riveted impellers from other rotors disallowed this premise. One of the leading authorities on the subject of impeller stress analysis agreed and suggested that

another technique be used where a theoretical analysis would be made of a finite element to confirm the expected stress level in the impeller. Because of the lack of any positive correlation of the proposed technique with measured stress levels, it was decided that the strain gauge data were as good as could be achieved under any circumstances.

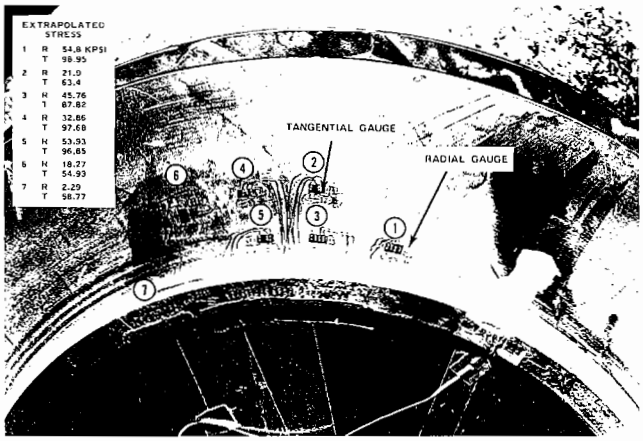

Figure 3. Gauge Locations for Stress Analysis.

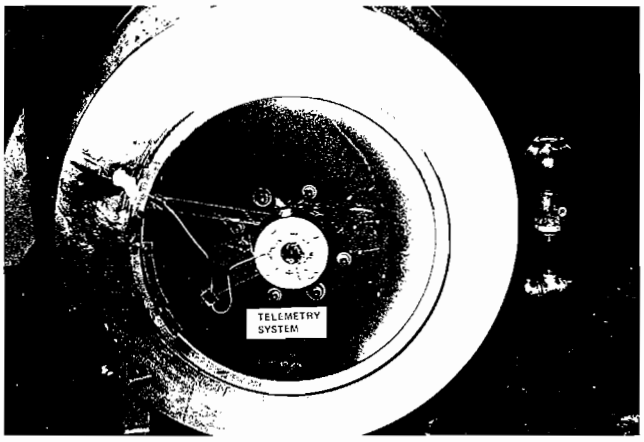

Figure 4. Telemetry System for Strain Gauges.

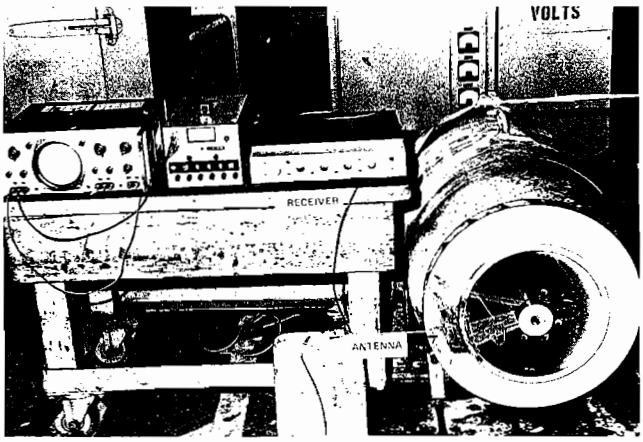

Figure 5. Test Set-up for Obtaining Stress Levels in Impellers.

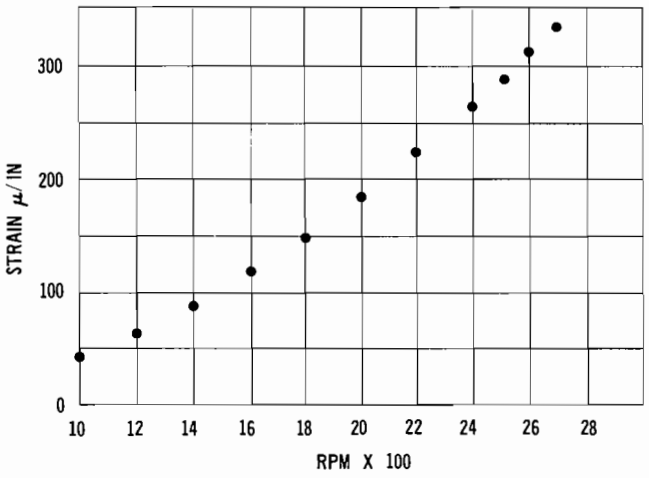

Figure 6. Effect of Speed on the Strain in First Stage Impeller.

Calibration of the strain gauge data was achieved by use of a static test device shown on Figure 7. Use of the small screw caused the test specimen to go in tension at the location of the strain gauge. With the gauge connected to the telemetry system, the required load was applied to generate approximately 303 microstrain, which was the approximate maximum impeller strain measured at 2,700 rpm. This was transmitted to the telemetry readout system. While in the strained position, the strain gauge leads were transferred from the telemetry system to a static strain meter. Initial loaded and subsequent unloaded strains were recorded and showed a differential of 287 microstrain. After both systems had been corrected for strain gauge factors, the final correlation indicated 286.5 microstrain on the telemetry system, which is remarkable agreement.

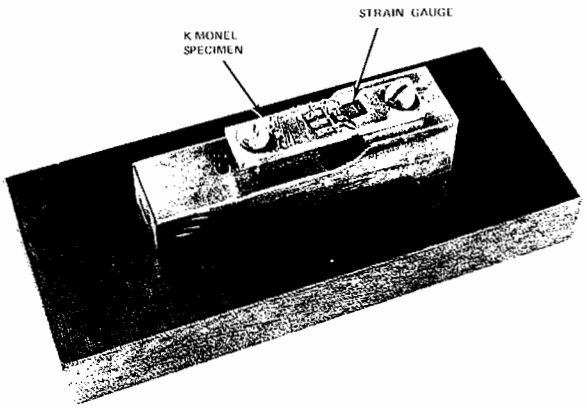

Figure 7. Static Test Device for Calibration of the Strain Gauge.

PRELIMINARY CONCLUSIONS

Based on the metallurgical report of the physical properties of the failed impeller, observation of the surface of the cracks and the stress analysis made and it was concluded that the first two failures had occurred for the following reasons:

1. The physical properties of the material had failed to come within design requirements (100,000 psi yield predicted; 65,000-73,000 psi observed depending on location).

2. The actual stress level at normal operating speed was significantly higher than expected. (Extrapolating the strain gauge data to running speed gave a tangential stress 99,000 psi compared to the 67,000 psi predicted.)

The combination of these two factors, plus a yet unidentified forcing function, caused the impeller to fail in a fatigue mode.

SUPPORTIVE TEST WORK

Subsequent to the stress analysis, another technique was attempted to see if the presence of hydrogen sulfide and water in the gas might accelerate the fatigue phenomenon. A test specimen cut from the cover of second failure impeller was arranged as shown on Figure 8. The bolt used to apply a tensile load to the specimen was bored to permit flow of hot and cold water. The test arrangement is shown on Figure 9. The timer was set to permit hot water to pass through the bolt for approximately one minute. This caused the bolt to expand. In this manner, additional tensile load was put on the test specimen. Subsequent to the heating cycle, cold water was passed through the bolt for 14 minutes allowing the coupon to return to its ambient preload of approximately 70,000 psi. This cycle loading was conducted with the test coupon emersed in a bath of hydrocarbon condensate removed from the compressor suction drum. The specimen was subjected to approximately 3,000 cycles. The stress level was increased approximately 8,000 psi with each heating cycle; no significant distress due to corrosion was found on the specimen after it was removed for examination. Further, samples that were stressed to 70,000 psi and put into a drum through which corrosive hydrocarbon condensate was continuously circulated showed no ill effects after approximately three months of emersion. This test arrangement is shown on Figure 10. All of these tests gave additional credibility to the premise that corrosion was not the prime factor in the failure of these impellers.

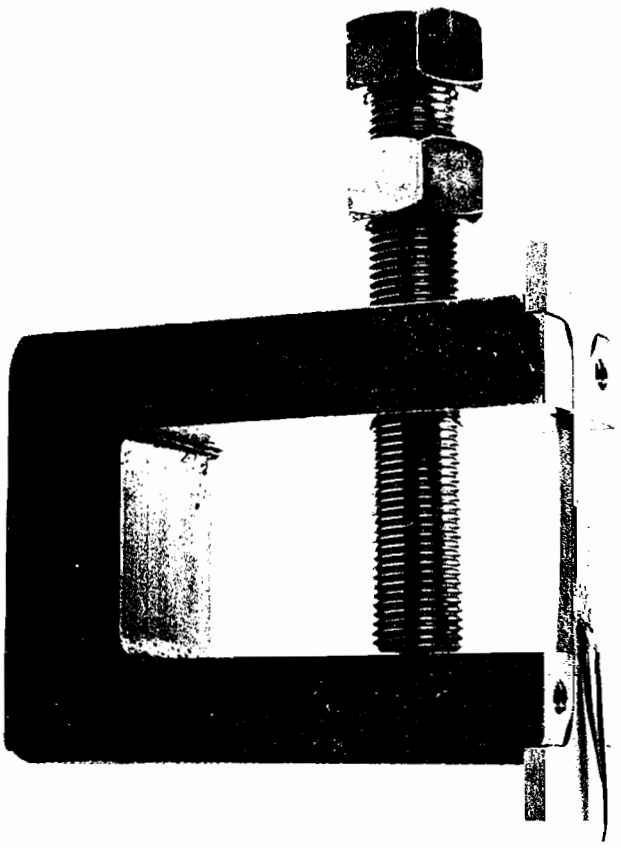

Figure 8. A Test Specimen Cut from the Case of a Second Failure Impeller.

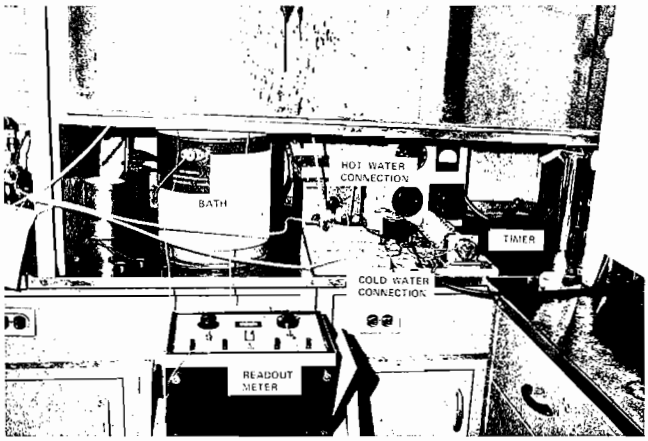

Figure 9. Test Arrangement Showing Application of Tensile Load.

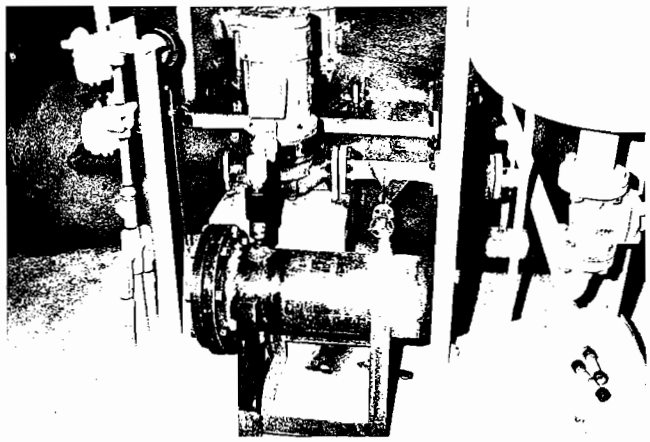

Figure 10. Test Arrangement Showing a Sample Being Stressed to 70,000 psi and Placed in a Solution of Corrosive Hydro-Carbon Condensate.

THE THIRD FAILURE

After the first SAE 4330, 90,000-maximum-yield, first-stage impeller had been in service approximately eight months, it was removed from service during a scheduled downtime of the process unit. The overall performance of the compressor had dropped below the "like new" performance. This, combined with the lack of operating data with the SAE 4330 material in this wet gas service, dictated an inspection of the rotor. Figure 11 shows the condition of the first-stage impeller as it was found during this inspection. It should be noted that there are three cracks present; two appear to be approximately 180 degrees from the large single crack. The two cracks are in adjacent vanes. The main crack followed the back side trailing edge of the vane as shown on Figure 12.

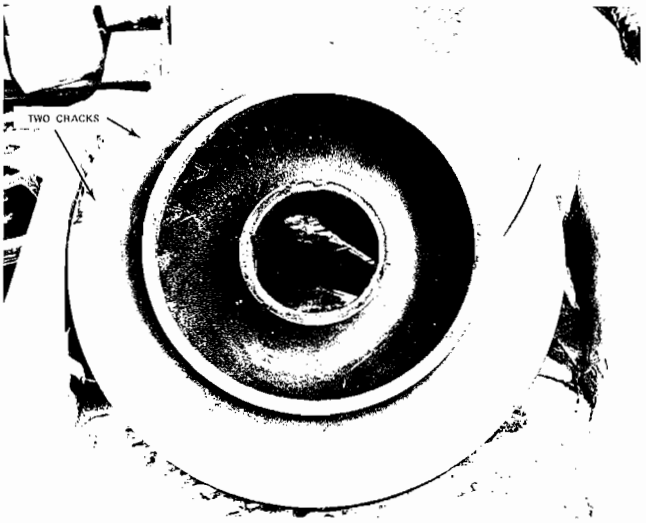

Figure 11. Condition of First Stage Impeller During Inspection; After Eight Month Service.

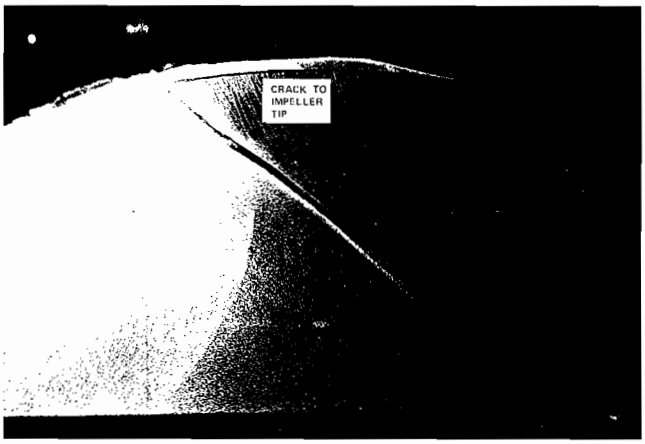

Figure 12. Crack on the Back Side of the Trailing Edge of the Vane.

It was suggested that this impeller be put on the shaker table to establish its natural frequency in its failed condition. However, due to the pressing need for metallurgical examination, this test was not performed, and the impeller was cut into sections to permit examination of the cracks. Close examination of the inlet side of the impeller hub showed rather severe corrosion/erosion to have taken place. A comparison of the same area on K-Monel and SAE 4330 material is shown on Figures 13 and 14. As can be seen, the original machining marks are still visible on the K-Monel. The SAE 4330 material had less on-line service time than the K-Monel. No significant process difference had been observed during the operating of the SAE 4330 material. This inspection confirmed our original selection of the use of K-Monel for this service.

It was rather refreshing to review the metallurgic analysis made by both the vendor and our research affiliate. Both had concluded that the failed SAE 4330 material had the proper physical properties (tensile and hardness). Examination of the fractured surface indicated the crack had been manifest for quite some time. There were some indications that fatigue had taken place. It was a personal judgment that suggested the impeller had failed in fatigue, but in doing so, had detuned itself and thus was less responsive to the unknown stimulus. This is the first time that serious thought was given to the possibility of the presence of a forcing function. Having this type of failure in this short time period with the nominal stress levels known to be within design limits, suggested that some additional forcing function must exist. At that time, it was not known whether it was one of short duration with high stress levels, or one that was manifest for an extended period with low stress levels. Because of the start and stop mode of operation that we were still experiencing due to turbine fouling problem, credibility was given to the former premise. Prior to the installation of the spare SAE 4330 rotor, an accelerometer was mounted on the disc of the impeller. By striking the impeller, it was made to ring at a multiple frequency range. This signal was recorded on magnetic tape and found to have a primary frequency of approximately 560 cycles per second. The vibration could still be seen on an oscilloscope despite the fact that the sound had dropped below the audible level.

Figure 13. K-Monel Hub After 282 Days Service.

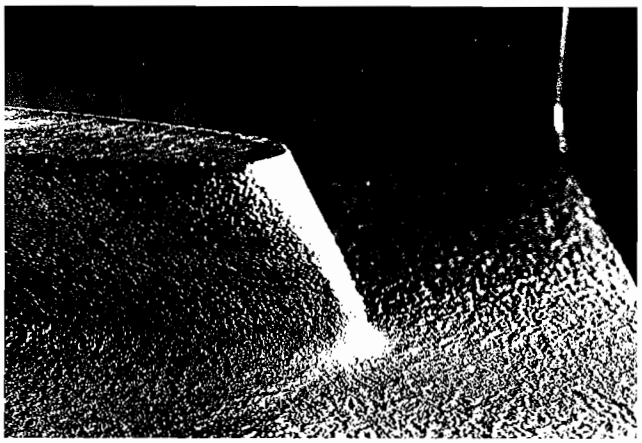

Figure 14. SAE 4330 Hub and Vane After Ten Months Service.

BEHAVIOR IN SURGE

The ringing test did show the responsiveness of the impeller to a stimulus. After the impeller was put into service, the compressor casing was equipped with the following:

1. In the area of the inlet nozzle, the following were mounted:
   A. An accelerometer.
   B. A velocity pick-up.
   C. A pressure transducer was inserted to the inner surface of the inlet casing.
2. The compressor was already equipped with a noncontacting probe used to monitor normal shaft vibration and tachometer to provide a timing pulse.

This equipment was used to observe the behavior of the compressor in surge, and to ascertain the device best suited to detect or predict surge.

The compressor was put into surge by slowing it down. The resulting phenomena were recorded simultaneously on magnetic tape and are shown on Figure 15. As can be seen, the noncontacting probe indicated an apparent drop in shaft speed from 7,000 cpm to approximately 3,500 cpm when actually the speed had been reduced only 200 cpm. Further, the amplitude of the shaft radial vibration increased approximately 400 percent. At the same time, the pressure in the inlet casing was observed to rise substantially. Also, acceleration and velocity levels showed substantial increases. Reducing the tape speed from 30 inches per second to 3-7/8 inches per second, a 7.74 to 1 step down showed these phenomena more clearly (Figures 16A, B, C, and D). The magnetic tape was also used in conjunction with a realtime analyzer. The presence of a very strong 560-cycles-per-second frequency was indicated. This is shown on Figure 17. It could be concluded that during this surge period, which lasted for 1.5 seconds, the back flow of gas generated white noise. One of the very strong frequencies in this noise was in the league of the same 560-cycles-per-second frequency mentioned earlier. This procedure was repeated at least five times to obtain additional data. Each time, some new information was observed. All the data point to the conclusion that the unknown forcing function was acoustically generated during surge. This caused the first-stage impeller to vibrate in a manner that caused the fatigue phenomena to become manifest. Further, since no problems have been experienced with the other five impellers, it was decided that all future efforts would be directed toward developing better understanding of the vibratory characteristics of the first-stage impeller and their relationship to the acoustical phenomena present during surge.

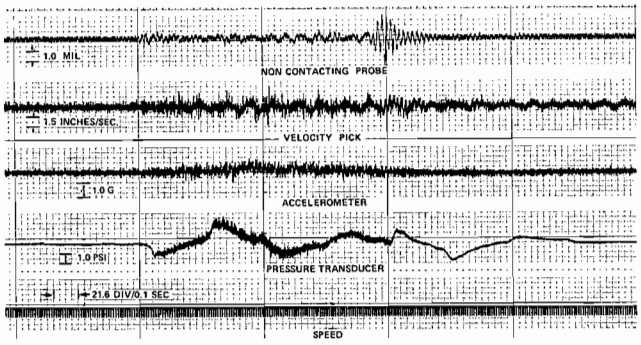

Figure 15. Compressor Analysis: Data as Unit is Approaching Surge.

ADDITIONAL TEST WORK

In an attempt to further define a responsiveness of this impeller, it was sent to an independent research facility to confirm its natural frequency. This was done by using an oscillator with an amplifier driving the impeller. It was interesting to note that as a prelude to the shaker test, the noncontacting probe, accelerometer, and strain gauges all gave essentially the same type of information over the same spectrum. Analysis of all the spectra indicated 560 cycles per second to be the very dominant frequency. As a final step, the impeller was placed on a shaker table and stimulated at the apparent sensitive frequencies. For purposes of understanding the display, the impeller was painted black. The location of the vanes are shown by the white lines. The most predominant frequency was in the league of 539 cycles per second, which is shown on Figures 18 and 19. Both figures show the two-diameter mode sensitivity of the impeller. From this, it was concluded that during surge, the rotor was being stimulated in such a manner as to give rise to a very strong bending mode with the attendant high cyclie stresses that caused the fatigue failure to occur.

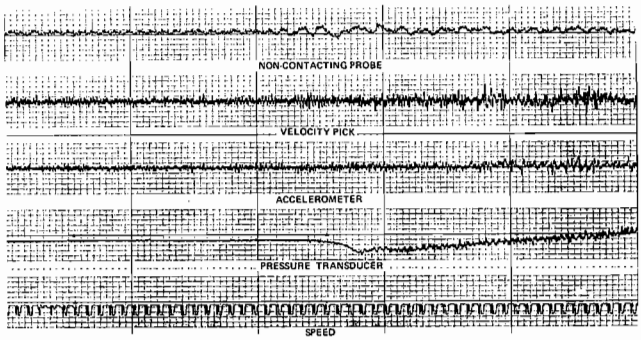

Figure 16a. Compressor Analysis Data as Compressor is Approaching Surge; at Reduced tape Speed.

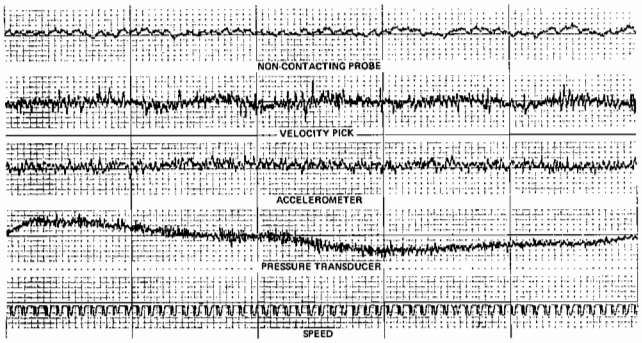

Figure 16b. Compressor Analysis Data as Compressor is Approaching Surge; at Reduced tape Speed.

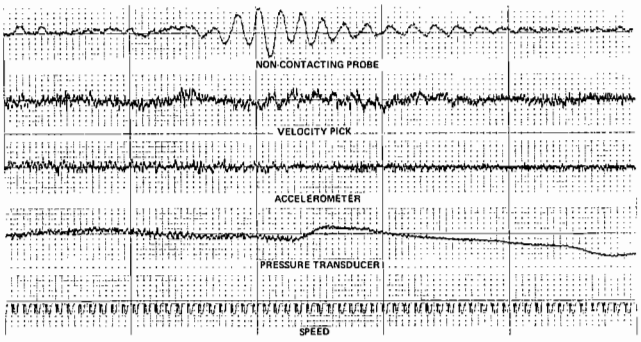

Figure 16c. Compressor Analysis Data as Compressor is Approaching Surge; at Reduced tape Speed.

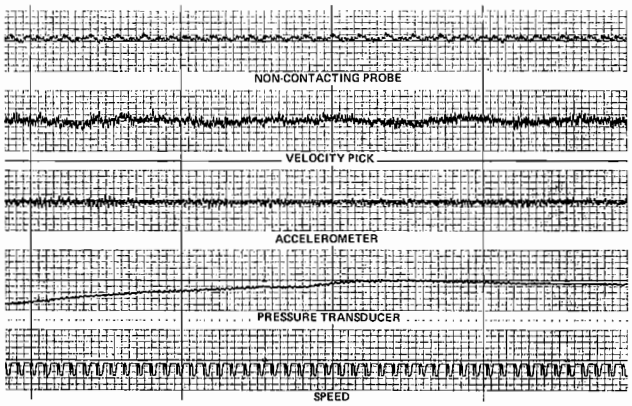

Figure 16d. Compressor Analysis Data as Compressor is Approaching Surge; at Reduced tape Speed.

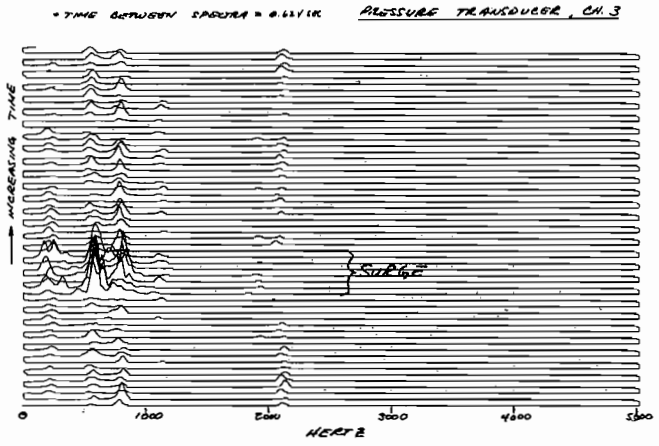

Figure 17. Real Time Analysis of Surge.

Figure 18. Vane Location Relative to Cover.

Figure 19. Vane Location Relative to Disc.

SURGE — DID IT OCCUR DURING NORMAL OPERATION?

As mentioned in the opening comments of this paper, the compressors had been purchased for catalytic wet gas service with average molecular weight of 42. During the period prior to failures, numerous tests were run on the compressor to establish its compliance with the design specifications. During one period approximately three months prior to shutdown, a short period of surge was observed, and the machine had to be shut down because of a badly upset process unit. Further, because of mechanical difficulty on the process unit, tests showed that the gas composition had changed significantly during this period. The compressor was operating in an area that may have caused it to be more susceptible to surge. Recording data during several starts and stops of the compressors, it was noted that the most serious surge occurred during a rundown after a trip and not during start-up. Normally, a compressor with proper recycle facilities would come on line with the minimum amount of surging. However, during a shutdown, at least two hard surges occur prior to the compressor being shut in.

The test work mentioned above indicated a rather remarkable correlation between the presence of hydrogen in the gas stream and a change in the temperature across the compressor. At first, an attempt was made to correlate a change in K value of the gas and the presence of hydrogen and performance. However, because of the complex correlation curve generated, it was discarded in favor of a simple curve that shows the relation of Δ T and the amount of hydrogen present in the gas. This correlation is shown on Figure 20. It should be noted as the Δ T rose, the percentage of hydrogen also was found to increase. Utilization of a computer designed for machinery monitoring permitted close observation of the Δ T on each compressor. When this differential reaches a maximum of 225° F or the equivalent of 10 percent hydrogen, an alarm is now sounded that permits the operator to start taking remedial action to reduce the amount of hydrogen present in the wet gas going to the compressors. Using this technique, we have not experienced any surging since implementation of the program.

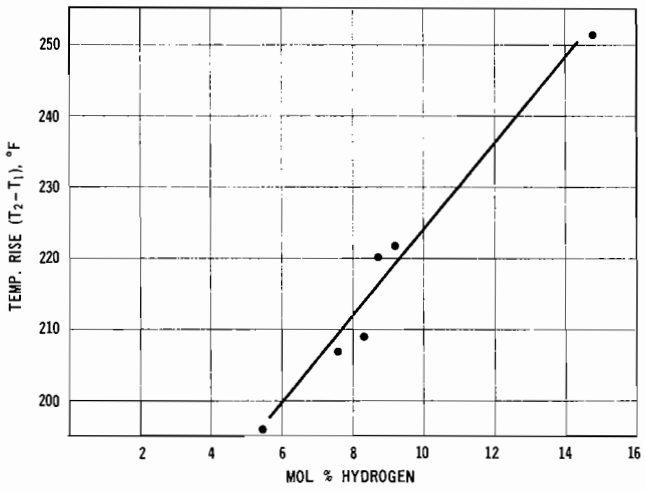

Figure 20. Wet Gas Composition Correlation.

ENGINEERING CONCLUSIONS

A substantial technical effort has been put forth in the field to try to identify the factors that could contribute to the failures. The procedures used during field test work included:

1. Use of electron beam scanning microscope to study the condition of the failed interface.
2. Use of strain gauges and telemetry.
3. Short-term fatigue and static strain specimen were tested in corrosive hydrocarbon bath to try to establish the effect of corrosion.
4. Recording of hydraulic and mechanical phenomena during surge.
5. Use of consulting facilities to provide specific expertise.
6. Both the noncontacting probe and a pressure transducer could be used to detect surge by monitoring with the existing machinery monitoring computer system.

It took all of the above to build the structure of what is now the failure analysis. The data point to surge as providing the stimulus in the form of noise. Several avenues are available that offer possible solution to this problem. These are:

1. *Reconstitute the Compressor*

   This would require rebuilding the compressor. Total capacity would be reduced, and this solution is unacceptable from a delivery capacity and economic standpoint.

2. *Monitor the Process to Minimize the Possibility of Surge*

   This is being done by the hydrogen versus Δ T correlation developed during the performance testing. The suction pressure will also be monitored. However, some surging will take place during normal starts and stops of the compressors and sudden process-oriented upsets.

3. *Reduce the Impeller Stress*

   A. The base line stress has been reduced by the speed reduction permitted by the addition of one stage. The additional stress resulting from surge will continue to remain.

   B. Redesign of the first stage to make it more serviceable during surge. This is now being reviewed.

4. *First Stage Must Be Made of K-Monel*

   Test work on the static/dynamic strain specimen and the condition of the first-stage, 90,000-maximum-yield impeller now dictate that K-Monel be used.

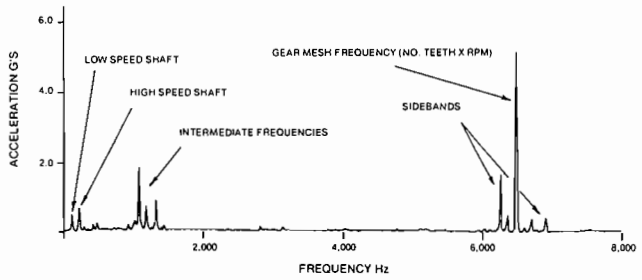

Figure 1. Vibration Signature of a Typical Industrial Double Helical Gear.

in Figure 1, a linear amplitude versus frequency spectrum plot, may be divided into three segments. First are the low frequencies containing running speeds and their harmonics up to approximately the 4th or 5th order. Next, in order of increasing frequency, is a segment beginning at the termination of the low frequencies and extending to a point in the spectrum just below the gear mesh frequency. As shown in Figure 1, a group of synchronous components are often found in this band at frequencies ranging from approximately 1,000 to 2,000 Hz. These components, hereafter designated intermediate frequencies, are likely associated with a resonance and, as will be discussed in later paragraphs, have been prime symptoms of deteriorating mechanical condition.

The final segment contains the gear mesh frequency (number of teeth multiplied by shaft speed) often surrounded by sidebands spaced at multiples of the rotational frequencies.

Although omitted from Figure 1 to enhance resolution, it is not uncommon for the gear mesh frequency to be followed by a harmonic series of its own as illustrated in Figure 2.

Likewise omitted from Figure 1 is the tooth repeat or hunting tooth frequency which may be produced when a deformed tooth or area on the gear meshes with a similarly deformed tooth or area on the pinion. The hunting frequency may be calculated from the following:

$$F_{tr}\,(Hz) = \frac{ng}{60Np}$$

ng = speed of the gear in RPM
Np = number of teeth on the pinion

Since the tooth repeat frequency occurs at such a low frequency, generally on the order of 1 Hz in industrial applications, it is seldom observed directly but rather as an amplitude variation of the gear mesh frequency.

As mentioned in a previous paragraph, the interpretation of low frequency vibration; running speed and low order harmonics, has been well defined. Element unbalance, misalignment and looseness are examples of problems likely to produce abnormal low frequency characteristics as are manufacturing errors such as pitch line or apex runout.

On the other hand the external characteristics of problems leading to pitting, scoring and possibly tooth fatigue are much more difficult to identify and evaluate. As an example, the gear mesh frequency is one of the primary acoustic characteristics of any gear, however, normal amplitudes vary widely from gear to gear and even on the same gear depending on load.

The signatures shown in Figure 2 illustrate an extreme example of load induced variations in the gear mesh frequency. Beginning with the top signature, recorded on the gear of a gas turbine generator at 15.5 MW, a significant decrease occurs as load is reduced to 9.5 MW, pictured in the middle signature.

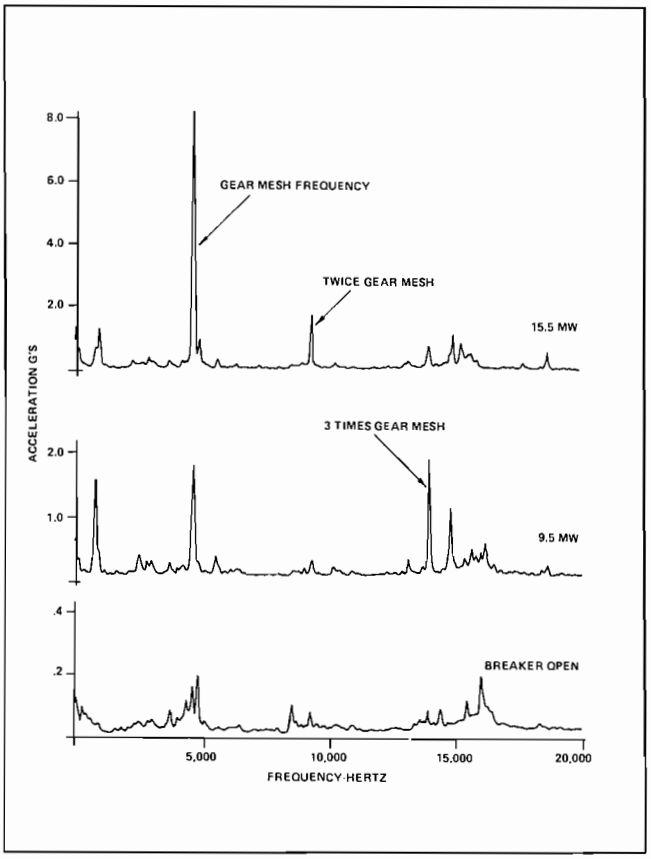

Figure 2. High Frequency Amplitude Variations Corresponding to Changes in Gear Load.

At synchronous speed and no load the gear mesh frequency has decreased to an amplitude less than its upper sideband as shown in the bottom signature.

In addition to relatively long term variations in amplitude at the mesh frequency, such as those caused by changes in load, there may be shorter term variations generated in the meshing process itself. Important from a diagnostic standpoint these short term variations represent deviations from a sinusoidal tooth engagement and are observed as sidebands around the mesh frequency as well as multiples of the mesh frequency.

At one time the position and relative strength of the mesh frequency sidebands were considered a promising indicator of gear condition. Later, more direct methods of subjecting the mesh process to detailed examination involves amplitude and frequency demodulation of the gear mesh frequency. The demodulated signal is then spectrum analyzed to produce a graphic representation of the dynamic variations occurring at mesh.

The theory behind this technique is quite simple. If the process of tooth engagement was purely sinusoidal the resulting mesh frequency would likewise be sinusoidal and hence represented by a single spectral component. Similarly, any deviation from a sinusoidal engagement will produce a corresponding variation in the mesh frequency. The hunting tooth error mentioned previously is a good illustration of this phenomena as it often produces an audible amplitude variation of the gear mesh frequency which may be easily clocked with a stop watch.